agronomy

MDPI

Article

Genetic Basis and Exploration of Major Expressed QTL *qLA2-3* Underlying Leaf Angle in Maize

Yonghui He [1,2,†], Chenxi Wang [1,†], Xueyou Hu [1,3], Youle Han [1], Feng Lu [1], Huanhuan Liu [1,2], Xuecai Zhang [4,*] and Zhitong Yin [1,2,*]

[1] Jiangsu Key Laboratory of Crop Genomics and Molecular Breeding/Key Laboratory of Plant Functional Genomics of the Ministry of Education/Jiangsu Key Laboratory of Crop Genetics and Physiology/Joint International Research Laboratory of Agriculture and Agri-Product Safety of the Ministry of Education, Agricultural College, Yangzhou University, Yangzhou 225009, China
[2] Jiangsu Co-Innovation Center for Modern Production Technology of Grain Crops, Yangzhou University, Yangzhou 225009, China
[3] Crop Breeding and Cultivation Research Institute, Shanghai Academy of Agricultural Sciences, Shanghai 201403, China
[4] International Maize and Wheat Improvement Center (CIMMYT), Mexico City 06600, Mexico
* Correspondence: xc.zhang@cgiar.org (X.Z.); ztyin@yzu.edu.cn (Z.Y.)
† These authors contributed equally to this work.

Abstract: Leaf angle (LA) is closely related to plant architecture, photosynthesis and density tolerance in maize. In the current study, we used a recombinant inbred line population constructed by two maize-inbred lines to detect quantitative trait loci (QTLs) controlling LA. Based on the average LA in three environments, 13 QTLs were detected, with the logarithm of odds ranging from 2.7 to 7.21, and the phenotypic variation explained by a single QTL ranged from 3.93% to 12.64%. A stable QTL, *qLA2-3*, on chromosome 2 was detected and was considered to be the major QTL controlling the LA. On the basis of verifying the genetic effect of *qLA2-3*, a fine map was used to narrow the candidate interval, and finally, the target segment was located at a physical distance of approximately 338.46 kb (B73 RefGen_v4 version), containing 16 genes. Re-sequencing and transcriptome results revealed that five candidate genes may be involved in the regulation of LA. The results enrich the information for molecular marker-assisted selection of maize LA and provide genetic resources for the breeding of dense planting varieties.

Keywords: leaf angle; maize; quantitative trait loci; QTL mapping

Citation: He, Y.; Wang, C.; Hu, X.; Han, Y.; Lu, F.; Liu, H.; Zhang, X.; Yin, Z. Genetic Basis and Exploration of Major Expressed QTL *qLA2-3* Underlying Leaf Angle in Maize. *Agronomy* **2024**, *14*, 1978. https://doi.org/10.3390/agronomy14091978

Academic Editor: Pedro Revilla

Received: 13 July 2024
Revised: 27 August 2024
Accepted: 30 August 2024
Published: 1 September 2024

1. Introduction

Appropriately reducing leaf angle (LA) is one of the most effective measures to increase maize planting density and yield [1,2]. The complete maize leaf is composed of a sheath, blade and ligular region. The ligular region is located at the junction of the sheath and leaf and is divided into two parts: the ligule and the auricle [3]. The ligule is close to the maize stem and can be regarded as an extension of the leaf sheath. By contrast, the auricle is located on either side of the mid-vein and has a wedge-shaped structure. The ligule and auricle engage each other and act as hinges to keep the leaf and stem at a certain angle called the LA [4].

The identification of genes regulating maize LA is mainly involved in transcriptional regulation and hormone signalling conducted using mutants [4–6]. Transcriptional regulation is one of the main regulatory pathways affecting angle size. *lg1*, *lg2*, *lg3* and *lg4* mutants have defective or absent ligules and auricles, resulting in minimal LA [7–9]. The SQUAMOSA promoter binding transcription factor LG1 regulates LA by affecting cell autonomy [9]. The bZIP transcription factor *LG2* gene is expressed earlier than *LG1* and may be involved in the initiation of the early leaf ligular region [8]. The function defects

of *LG3* and *LG4* encoding KNOX transcription factors lead to abnormal development of the leaf primordia meristem and abnormal leaf corner morphology [7]. In addition, defective transcription factors lead to cell ectopic expression of ligule and auricle, resulting in distorted and variable LA morphology, such as *wab*, *drooping leaf1* (*drl1*) and *drl2* [10,11]. Hormone-related genes are involved in the regulation of LA. Mutations in *Brd1*, the enzyme that catalyses the last step of brassinolide (BR) synthesis, cause leaf twist and LA deformation [12]. The mutation of the *NANA PLANT2* gene related to BR biosynthesis resulted in decreased BR levels, extreme dwarfing and increased LA [13]. A natural mutation of the BR C-22 hydroxylase gene exhibits upright upper leaves and smart-canopy architecture, which is a genetic resource for breeding high-density maize varieties [6].

LA is regulated by multiple quantitative trait loci (QTL). A large number of QTLs controlling LA in maize have been detected in different genetic populations [3,4]. Nine QTLs for LA were detected using 180 recombinant inbred lines (RILs) constructed by B73 and Mo17 [14]. Using genotyping-by-sequencing analysis, 17 QTL controlling LA were detected [15]. Fourteen QTLs controlling LA were identified by a four-way strategy using a four-way cross-population [16]. A total of 30 LA QTLs were detected by association and linkage analysis using a nested association mapping population [17].

Several maize LA-related genes, including *ZmTAC1*, *ZmCLA4*, *ZmILI1*, *ZmIBH1-1*, *ZmRAVL1* and *ZmBrd1*, were cloned by fine-mapping strategies [2,18–21]. *ZmTAC1* encodes a Poaceae protein with an unknown function and is homologous to rice *OsTAC1*. Sequence variation in the 5′-UTR of *ZmTAC1* affects the expression of *ZmTAC1*, which in turn affects LA size [21,22]. *ZmCLA4* encodes a gramineous protein that negatively regulates auxin transport and is homologous to the gene *LAZY1* that controls tiller angle in rice [20]. *ZmILI1*, *ZmIBH1-1* and *ZmRAVL1* encode transcription factors that affect LA by regulating the expression of genes, including hormone responses, cell differentiation and cell wall formation [2,18–20].

It is a feasible way to improve maize plant density by introducing superior alleles that control LA into maize varieties. After the introduction of the rare allele *UPA2* in teosinte, the LA of the maize cultivar Nongda108 was significantly reduced, resulting in a higher yield under dense planting conditions [2]. In the study, we identified a novel major QTL for LA in maize, *qLA2-3*, using genetic mapping of the population. *qLA2-3* was detected in all three environments and explained up to 12.31% of the phenotypic variation. Furthermore, fine mapping was used to narrow the mapping interval to 338.46 kb. Based on the maize reference genome, this region contains 16 genes. Five candidate genes were identified based on re-sequencing and transcriptome data. The results of this study should provide genetic resources for maize plant architecture improvement.

2. Materials and Methods

2.1. Plant Materials

The inbred lines LDC-1 and YS501 are the two parent inbred lines of a commercial maize hybrid Tianyu 88 which was released by our lab. LDC-1 and YS501 carry tropical and temperate germplasm, respectively. These two inbred lines exhibit a significant difference in leaf angle. LDC-1 shows a larger leaf angle than YS501. A single-seed descent method was used to develop RILs from the cross between LDC-1 and YS501. Briefly, F2 kernels were obtained by selfing F1 plants in the spring of 2016. Approximately 200 F2 plants were grown and selfed to obtain F3 ears in the winter of 2016. One kernel from each F3 ear was used to generate the F4 plant. Then, a similar procedure was employed for F4, F5, F6, F7 and F8 ears. Finally, 186 F9 RILs were obtained in the spring of 2019 [23]. The plants of the two parents and RIL populations were grown in three environments, respectively: the Ledong experimental field of Hainan (N: 18.73°, E: 109.17°) in the winter of 2019 (E1); an experimental field on the Wenhui Road campus of Yangzhou University (N: 32.40°, E: 119.40°) in the spring of 2020 (E2); and an experimental field on the Yangzijin Campus of Yangzhou University (N: 32.40°, E: 119.40°) in the summer of 2020 (E3). The soil at the Yangzhou experimental site was sandy loam, with the duration of sunshine ranging from

12 to 14 h. The average high temperature trend during spring sowing was 25–32 °C, and the average low temperature was 16–25 °C. During summer sowing, the average high temperature trend was 32–25 °C, and the average low temperature was 25–16 °C. The soil of the experimental field in Hainan was sandy, and the sunshine duration was approximately 12 h. The average high temperature trend was 30–28 °C, and the average low temperature was 21–17 °C. The RILs underwent planting in a randomised complete-block design, where the experiment was replicated twice for enhanced reliability.

Genotype recombinants were planted in experimental fields in the winter of 2020 (Hainan), the winter of 2021 (Hainan), the spring of 2022 (Yangzhou University) and the summer of 2022 (Zhenjiang City, N: 32.22°, E: 119.26°), respectively, for fine mapping. Ten maize plants were sown in the field where the row length was 2 m, the plant spacing was 0.2 m and the row spacing was 0.6 m. Field irrigation, fertilisation, weeding, and pest protection and management are the same as in the general field.

2.2. Investigation of Maize LA Phenotype

LA between stem and leaf above the ear was measured using a protractor at 15 day after pollination [2]. Five randomly selected plants from each line of the RIL population were measured for QTL mapping. The LA above the ear of all plants in the fine mapping plot was recorded, and the average LA was used for analysis.

2.3. Data Analysis

The descriptive statistical analysis, ANOVA and correlation analysis of the phenotypic data of the LA of the RIL population were performed using Excel 2016 and SPSS 21.0 software. The computation of broad-sense heritability (H^2) is formulated as $H^2 = Vg/(Vg + Vge/l + V\varepsilon/rl)$, encompassing the variance components of genotype (Vg), genotype–environment interaction (Vge), and random error (Vε), with r standing for the number of replicates and l for the number of environments.

2.4. QTL Mapping

A high-density linkage map of 2624 bin markers with an average genetic distance of 0.9 cM between the markers was constructed in our previous study [23,24]. QTL mapping of average LA was performed using WinQTL Cartographer 2.5 software. The recombination rate was converted to genetic distance using the Kosambi function. With a walking step of 1.00 cM, the composite interval mapping method was used to obtain the logarithm of odds (LOD) of QTL by 1000 permutations ($p < 0.05$). LOD thresholds greater than 2.5 were considered significant QTL, and the prediction confidence interval was based on a drop interval of 1.5 LOD. The naming rules for QTLs were as follows: 'q' stands for QTL, followed by the LA abbreviation (LA), followed by the sequence number of the chromosomes, and finally, sorted according to their physical location on the chromosome.

2.5. Genome Re-Sequencing

Genomic DNA was extracted from two parental inbred lines, LDC-1 and YS501, and randomly interrupted by a Covaris crusher with a growth rate of 350 bp. The DNA library was constructed using the TruSeq Library Construction Kit and sequenced on the Illumina platform in strict accordance with the instruction manual (Novogene Co., Ltd., Beijing, China). Clean data obtained by removing adapters, poly-N sequences and low-quality reads were then mapped to the reference genome B73 RefGen_v4 (ftp://ftp.ncbi.nlm.nih.gov/genomes/all/GCF/000/005/005/GCF_000005005.2_B73_RefGen_v4, accessed on 29 August 2024) using BWA software (v0.7.8-r455) with default parameters. SAMtools (v1.3.1, parameters as mpileup -m 2 -F 0.002 -d 1000) was used to filter SNP/InDel detection criteria as follows: (1) the depth of the variate position is not less than 4; (2) the mapping quality is not less than 20 [25].

2.6. Fine Mapping of qLA2-3

InDel markers in or near the *qLA2-3* region were designed using a primer design tool (https://www.ncbi.nlm.nih.gov/tools/primer-blast/, accessed on 29 August 2024) to screen for genotype recombinant plants in the residual heterozygous lines (Table S1).

The recombinants in the *qLA2-3* interval were planted into plots after self-crossing for fine mapping in each generation. Each plot has over 100 plants used for measuring leaf angle data. The *qLA2-3* locus was mapped by analysing the genotype of each plant and its corresponding average LA in the plot. The significant difference in LA between the two parental homozygous genotypes indicates that the candidate gene is located in the heterozygous region; otherwise, it is located in the homozygous region.

2.7. RNA-Seq and qPCR

RNA samples were collected from the newly formed ligular region of the third leaf above the ear. The ligular regions of 15 plants were mixed into one sample, and three biological replicates were prepared for *qLA2-3*-NIL^{YS501} and *qLA2-3*-NIL^{LDC-1}. The total RNA in each sample was extracted with a Plant Total RNA Isolation Kit (Vazyme Biotech, Nanjing, China), as referenced in the user manual. The sequencing libraries were constructed using the NEBNext Ultra II RNA Library Prep Kit for Illumina (New England Biolabs, Ipswich, MA, USA) with reference to the standard operating manual. Clean reads were obtained from raw reads after filtering, such as removing 3′ end adapters (the removed part had at least a 10 bp overlap with the known adapter, allowing for 20% base mismatches) and low-quality data (reads with an average quality score lower than Q20) using Cutadapt (v1.11). Reads were mapped to the maize B73_RefGen_v4 reference genome (https://www.maizegdb.org/, accessed on 29 August 2024) using the HISAT2 (v2.1.0) software (http://ccb.jhu.edu/software/hisat2/index.shtml, accessed on 29 August 2024) under the condition of default parameters. The Read Count values mapped to each gene were counted and regarded as the original expression levels of the genes using HTSeq (v0.9.1). In order to make the gene expression levels among different genes/samples comparable, FPKM (Fragments Per Kilobases per Million fragments) was used to normalise the expression levels after excluding rRNA and tRNA (Personalbio Co., Ltd., Shanghai, China). Genes with expression fold changes exceeding 1.5 ($p < 0.05$) were considered significant differentially expressed genes by DESeq (v1.38.3).

For the qPCR analysis, 1 μg of total RNA was used to synthesise cDNA with an ABScript III RT Master Mix for qPCR (ABclonal, Wuhan, China) in accordance with the manufacturer's instructions. Gene fragments were amplified with Universal SYBR Green Fast qPCR Mix (Abclonal, Wuhan, China) on an ABI StepOnePlus Real-Time PCR system. The ΔCt (threshold cycle) method was used to determine the gene expression levels, and the expression of Maize *ZmGAPDH* (GRMZM2G046804) was taken as the internal control.

3. Results

3.1. Phenotypic Variation in LA Traits

Maize LDC-1 and YS501 inbred lines have similar plant heights but contain a large difference in upright plant architecture. Compared to LDC-1, YS501 showed 4.3°, 5.8°, 17.6°, 16.0°, 18.4°, 18.1° and 17.2° reductions in the first leaf below ear, leaf at ear position, first leaf above ear, second leaf above ear, third leaf above ear, fourth leaf above ear and fifth leaf above ear, respectively (Figure 1A,B). Significant differences in LA between the two parents were observed in all three environments, with parent YS501 containing a larger LA than parent LDC-1 (Table 1). Based on 186 RILs constructed with these two parents, the LA of the genetic mapping population was measured and analysed.

Agronomy **2024**, *14*, 1978 5 of 13

larger LA than parent LDC-1 (Table 1). Based on 186 RILs constructed with these two parents, the LA of the genetic mapping population was measured and analysed.

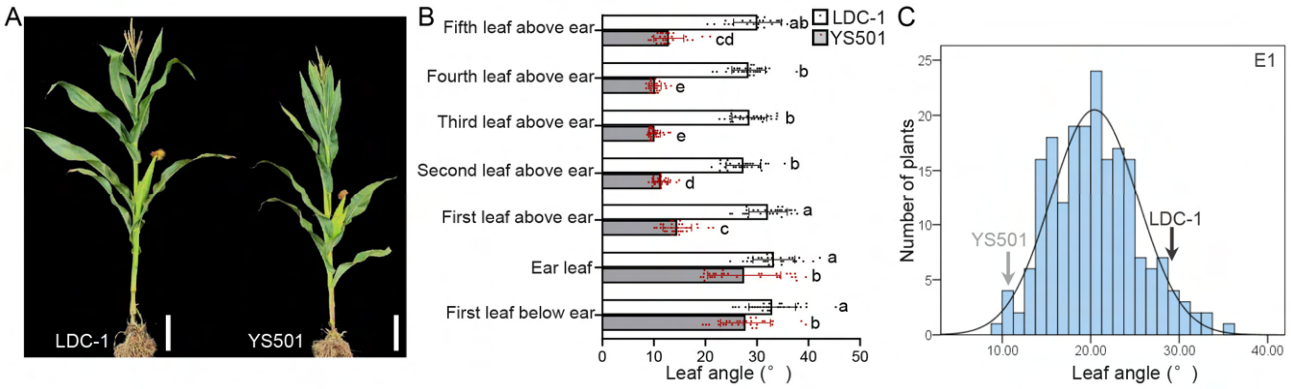

Figure 1. Phenotypic distributions of leaf angles in LDC-1, YS501 and RIL populations. (**A**) Comparison of leaf angles between LDC-1 and YS501. The scale bar was 20 cm. (**B**) Statistical data on leaf angle size between LDC-1 and YS501. $n = 30$; mean compassion letters represent significant differences at $p < 0.05$ level through Tukey's Honest Significant Difference Test. (**C**) Frequency distributions of mean leaf angle above the ear in the RIL population. The data in the E1 environment were used as an example. The X-axis represents the range of leaf angle distribution on the ear within the RIL population, the Y-axis represents the frequency, and the black line represents the normal distribution fitting curve.

Table 1. Phenotypic statistics of the leaf angle in parents and RIL population.

Environment	Parents			RIL Population						
	YS501	LDC-1	*t*-Test *p* Value	Mean ± SD	Range	Kurtosis	Skewness	*CV* (%)	*F* Value	H^2
E1	11.83	28.87	3.56×10^{-30}	20.33 ± 4.84	9.22–35.02	−0.043	0.331	23.81		
E2	10.25	26.97	1.01×10^{-30}	19.96 ± 6.41	9.07–37.54	0.389	0.429	32.11	8.216***	89.15%
E3	11.34	23.89	2.48×10^{-07}	22.50 ± 5.09	9.62–38.69	0.15	0.109	22.62		

SD, standard deviation; *CV*, coefficient of variation; H^2, broad-sense heritability. *** indicates extremely significant correlation at the $p < 0.01$ level.

The correlation analysis of the LA of the RIL population in three environments showed a considerably significant positive correlation ($p < 0.01$). In E1, E2 and E3 environments, the LA correlation coefficients of each leaf were 0.456–0.749, 0.515–0.812 and 0.450–0.729, respectively (Figure 2). The results of correlation analysis indicated that the genes regulating the LA of five leaves on the ear might have similar genetic regulatory mechanisms, so the average LA was used for further analysis.

Descriptive statistics show that the absolute values of skewness and kurtosis of LA in all environments were less than 1, suggesting that the data of LA present the characteristics of a normal distribution (Table 1). The coefficients of variation in LA in the three environments were 23.81%, 32.11% and 22.62%, respectively, with a large range of variation. The average LA of the RIL population was between that of parents, but there were also a number of lines whose LA was lower or higher than that of parents, showing transgressions (Figures 1C and S1). The genotype *F* value indicated that the genetic difference of LA reached a considerably significant level, and the broad sense heritability of LA was high, reaching 89.15%. These results indicate that the LA has a quantitative character and can be used for QTL mapping.

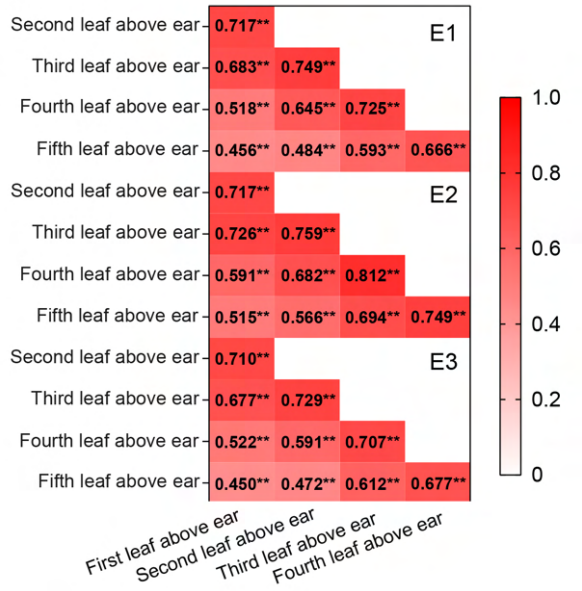

Figure 2. Correlation analysis of leaf angles on ears in the RIL population under three environments. E1: **Ledong** Experimental Base in Hainan in the winter of 2019–2020; E2: Maize Genetic Breeding Experimental Field in the Agricultural College of Yangzhou University in the spring of 2020; E3: Yangzhou University Experimental Farm in the summer of 2020. ** indicates an extremely significant correlation at the $p < 0.01$ level.

3.2. Identification of QTLs for LA

The average LA of each line was used as phenotypic data for the initial mapping of QTL regulating LA based on a high-density linkage map [24]. A total of 13 QTLs were identified in the three environments, which were distributed on chromosomes 1, 2, 3, 4, 5, 6, 7, and 10 (Table 2). Each QTL explained 3.93%–12.64% of phenotypic variation and had LOD values between 2.7 and 7.21.

Table 2. Quantitative trait loci (QTLs) for leaf angle detected using 186 recombinant inbred lines in three environments.

Trait	QTL	Chr	Position (cM)	Physical Location (bp)	E1 LOD	E1 Add	E1 R^2	E2 LOD	E2 Add	E2 R^2	E3 LOD	E3 Add	E3 R^2
LA	*qLA1-1*	1	115.1~135.1	37490781~57754942				7.21	2.33	12.64			
	qLA1-2	1	193.0~209.4	105544639~166628038	4.50	1.32	7.22						
	qLA1-3	1	349.7~371.2	281040428~292905589							3.45	1.20	5.27
	qLA2-1	2	55.8~67.6	12495796~16391990	3.86	1.30	6.98						
	qLA2-2	2	144.5~152.5	187673664~191462633							4.83	1.46	7.09
	qLA2-3	2	180.1~196.6	214012471~225807350	6.88	1.65	10.90	7.03	2.37	12.31	4.30	1.39	6.25
	qLA3-1	3	13~18.9	2050621~3087150	3.08	1.12	4.87						
	qLA3-2	3	147.2~153.8	181135621~184419019							3.12	1.09	4.57
	qLA4-1	4	180.4~195.1	208732552~236286534				3.69	1.67	6.25			
	qLA5-1	5	113.3~116.6	61422142~67028398							3.27	−1.07	4.34
	qLA6-1	6	82.6~95.0	116217831~136871955							4.31	1.47	7.44
	qLA7-1	7	231.3~238.7	155068009~170104806							2.70	−1.02	3.93
	qLA10-1	10	53.8~69.6	13051133~30669331	3.97	1.54	9.45						

LA, leaf angle; Chr, chromosome; LOD, logarithm of odds; Add, additive effect value; R^2, phenotypic contribution rate.

The average LA of each line was used as phenotypic data for the initial mapping of QTL regulating LA based on a high-density linkage map [24]. A total of 13 QTLs were identified in the three environments, which were distributed on chromosomes 1, 2, 3, 4, 5, 6, 7, and 10 (Table 2). Each QTL explained 3.93%–12.64% of phenotypic variation and had LOD values between 2.7 and 7.21.

Among QTLs, *qLA2-3* on chromosome 2 was detected in all three environments (Figure 3A). The genetic effect of *qLA2-3* was the largest, accounting for 10.90%, 12.31%, and 6.25% of the phenotypic variation, and the synergistic allele originated from LDC-1 (Table 2). The physical location of *qLA2-3* was 214.0–225.8 Mb (genetic locus 180.1–196.6 cM), and there was no reported gene related to LA in this region.

qLA10-1	10	53.8~69.6	15031133~90669531	5.97	−1.54	9.45

LA, leaf angle; Chr, chromosome; LOD, logarithm of odds; Add, additive effect value; R^2, phenotypic contribution rate.

Among QTLs, *qLA2-3* on chromosome 2 was detected in all three environments (Figure 3A). The genetic effect of *qLA2-3* was the largest, accounting for 10.90%, 12.31% and 6.25% of the phenotypic variation, and the synergistic allele originated from LDC-1 (Table 2). The physical location of *qLA2-3* was 214.0–225.8 Mb (genetic locus 180.1–196.6 cM), and there was no reported gene related to LA in this region.

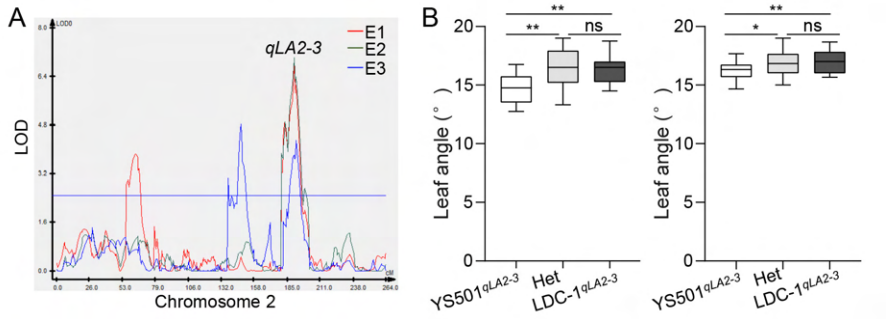

Figure 3. The main QTL locus, *qLA2-3*, for leaf angle detected on chromosome 2. (**A**) Logarithm of odds (LOD) figure for *qLA2-3*. The X-axis is the genetic distance on each chromosome, the Y-axis is the LOD value of the QTL, and the middle horizontal line represents the threshold (LOD = 2.5). (**B**) Allele effects of *qLA2-3* for leaf angle in two plots. * indicates significant difference at the $p < 0.05$ level; ** indicates significant difference at the $p < 0.01$ level; ns indicates no significant difference.

3.3. Validation and Fine Mapping of *qLA2-3*

To obtain progeny plants with heterozygous genotypes in the major QTL *qLA2-3* region, recombinants with the LDC-1 allele were backcrossed to YS501 and planted into plots after self-crossing. The genetic effect of *qLA2-3* was validated by identifying the genotypes and average LAs of each plant (Figure 3B). Compared to the LDC-1 allele, the YS501 allele at *qLA2-3* reduced the LA.

The major QTL, *qLA2-3*, was located between the initial location markers AX-90526710 and AX-86258763. Within or near the two markers, 12 InDel markers were developed to determine the recombination sites of the genotypes (Figure 4). Based on the genotype and phenotype data of six recombinant plant progeny plots, the mapping interval was narrowed to between markers YS54 and YS11. According to reference genome information for B73 RefGen_v4, the physical distance was approximately 3.87 Mb (Figure 4B). Subsequently, the offspring of seven identified recombinants were planted in isolated plots. Based on new InDel markers such as YS4, YS5, A0, LD21, B10 and A9 developed in the interval, the location interval is further narrowed to between markers YS4 and YS5, with a physical distance of approximately 338.46 kb (Figure 4C).

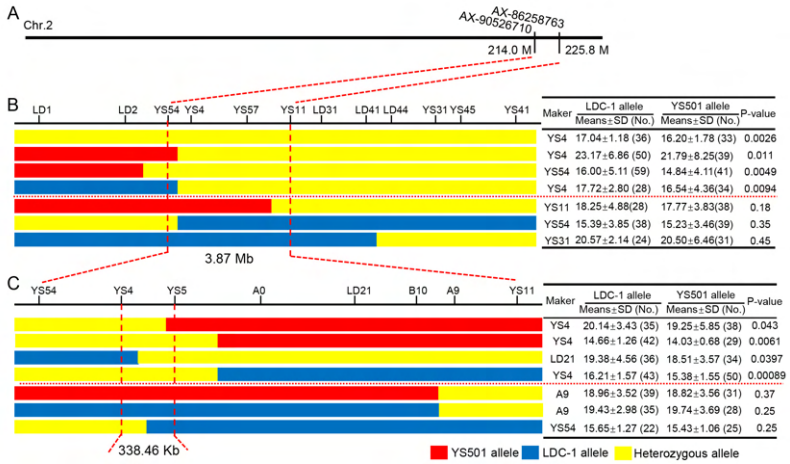

Figure 4. Fine mapping of *qLA2-3* based on recombinant progeny: (**A**) Schematic diagram of the pre-mapping region of *qLA2-3*. (**B**) The genotypes and LA phenotypes of recombinant in the spring of 2022 in Yangzhou. (**C**) The genotypes and LA phenotypes of recombinant in the summer of 2022 in Zhen-jiang. Red, blue and yellow represent homozygous YS501, homozygous LDC-1 and heterozygous YS501/LDC-1 alleles, respectively. Marker, genotype information for statistical analysis; No, the number of individuals in the planting plot. The red dashed line is used to mark the positioning interval. The red dotted line is used to distinguish between significant and insignificant data.

To verify the allelic effects of *qLA2-3* in the localised region, a pair of near isogenic lines (*qLA2-3*-NIL^{YS501} and *qLA2-3*-NIL^{LDC-1}) was developed from a RIL that was heterozygous in the 338.46 kb region. Compared to *qLA2-3*-NIL^{LDC-1}, *qLA2-3*-NIL^{YS501} decreased by 0.97°, 2.46°, 3.64° and 4.68° from the first to the fourth leaf above the ear, respectively, and the average LA decreased by 2.51° (Figure 5A,B). There were significant differences in every LA between the two NILs, and alleles from YS501 had a smaller LA.

In addition to LA, plant height, ear height, leaf length and leaf width are relevant traits of upright plant architecture. Six traits, including plant height, ear height, tassel length, number of tassel branches, leaf length and leaf width, were also investigated in the *qLA2-3*-NIL^{YS501} and the *qLA2-3*-NIL^{LDC-1}. Compared to *qLA2-3*-NIL^{LDC-1}, the leaf width of *qLA2-3*-NIL^{YS501} was significantly reduced by 0.51 cm, but no significant difference was

3.4. Evaluation of the Influence of qLA2-3 on Upright Plant Architecture

To verify the allelic effects of *qLA2-3* in the localised region, a pair of near-isogenic lines (*qLA2-3*-NIL^{YS501} and *qLA2-3*-NIL^{LDC-1}) was developed from a RIL that was heterozygous in the 338.46 kb region. Compared to *qLA2-3*-NIL^{LDC-1}, *qLA2-3*-NIL^{YS501} decreased by 0.97°, 2.46°, 3.64° and 4.68° from the first to the fourth leaf above the ear, respectively, and the average LA decreased by 2.51° (Figure 5A,B). There were significant differences in every LA between the two NILs, and alleles from YS501 had a smaller LA.

Agronomy **2024**, *14*, 1978 9 of 14

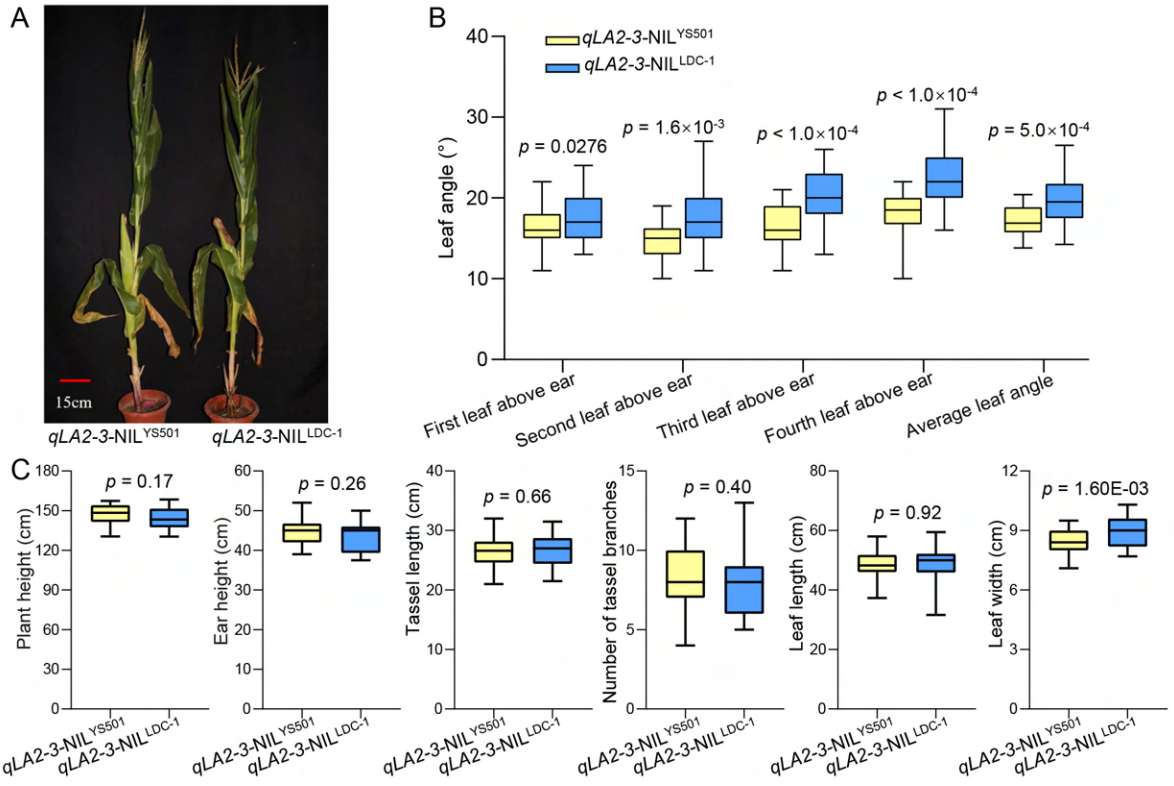

Figure 5. Comparisons of the leaf angle and agronomic traits between *qLA2-3*-NIL^{YS501} and *qLA2-3*-NIL^{LDC-1}. (**A**) The appearance of *qLA2-3*-NIL^{YS501} and *qLA2-3*-NIL^{LDC-1} at the maize filling period. Bar = 15 cm. (**B**) Statistical data of leaf angle between *qLA2-3*-NIL^{YS501} and *qLA2-3*-NIL^{LDC-1}. (**C**) Effect analysis of *qLA2-3* on plant architecture traits between *qLA2-3*-NIL^{YS501} and *qLA2-3*-NIL^{LDC-1}. $p < 0.05$ indicates a significant difference, $p < 0.01$ indicates an extremely significant difference.

3.5. Predicted Candidate Genes by Genome Re-Sequencing Analysis and Transcriptome Analysis

To narrow down the candidate genes in *qLA2-3*, the genomic variation was compared using re-sequencing data from the two parental lines. The comparison rate of samples ranged from 98.82% to 98.92%, the average coverage depth of reference genomes was 30.38× (LDC-1) to 31.92× (YS501), and the 1× coverage (covering at least one base) was above 91.34%, which could be used for mutation detection. After rigorous filtering, 906 polymorphic SNPs and InDel were detected between the two parents, YS501 and LDC-1, in this candidate region (Figure 6A and Data Set S1). There are 6.53% (59), 5.20% (47), 3.77% (34), 5.87% (53) and 0.11% (1) variants distributed in the exon, upstream, 5′-UTR, 3′-UTR and splicing regions, respectively, except 75.16% in the inter-genic regions (55.04%, 497), introns (16.28%, 147) and downstream sequences of coding regions (4.10%, 37), which are difficult to cause functional variation.

In addition to LA, plant height, ear height, leaf length and leaf width are relevant traits of upright plant architecture. Six traits, including plant height, ear height, tassel length, number of tassel branches, leaf length and leaf width were also investigated in the *qLA2-3*-NIL^{YS501} and *qLA2-3*-NIL^{LDC-1} parental lines. The comparison rate of samples ranged from 98.82% to 98.92%, the average coverage depth of reference genomes was 30.38× (LDC-1) to 31.92× (YS501), and the 1× coverage (covering at least one base) was above 91.34%, which could be used for mutation detection. After rigorous filtering, 906 polymorphic SNPs and InDel were detected between the two parents, YS501 and LDC-1, in this candidate region (Figure 6A and Data Set S1). There are 6.53% (59), 5.20% (47), 3.77% (34), 5.87% (53) and 0.11% (1) variants distributed in the exon, upstream, 5′-UTR, 3′-UTR and splicing regions, respectively, except 75.16% in the inter-genic regions (55.04%, 497), introns

(16.28%, 147) and downstream sequences of coding regions (4.10%, 37), which are difficult to cause functional variation.

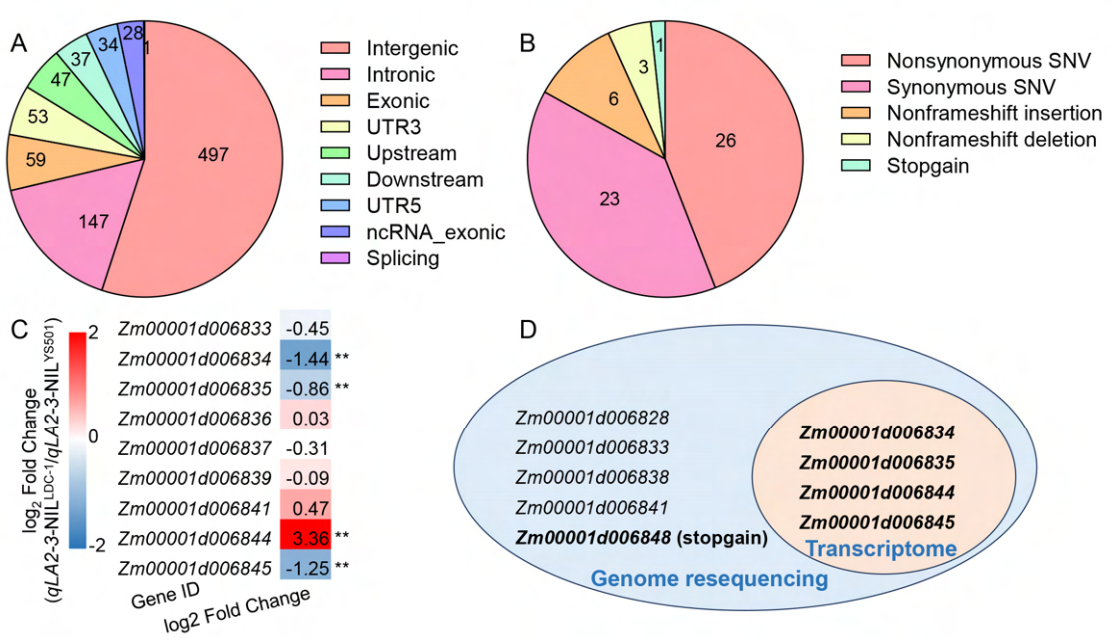

Figure 6. Genomic variation and gene expression changes in the *qLA2-3* candidate regions. The genomic distribution of variations in the leaf angle main QTL *qLA2-3* candidate regions (**A**) and mutation type in exonic regions (**B**). (**C**) Heatmap showing the gene expression changes in *qLA2-3*-NIL^{YS501} and *qLA2-3*-NIL^{LDC-1}. ** indicates significant difference at the $p < 0.01$ level. (**D**) Venn diagrams showing the predicted candidate genes in genome re-sequencing and transcriptome analysis. Nine genes had exons with variable sequences caused by SNPs or Indel in genome re-sequencing, and four of them were differentially expressed genes in transcriptional sequencing.

Among the sequence variations in the coding region, 23, 6 and 3 SNPs or InDel caused synonymous mutations, non-frameshift insertion or non-frameshift deletion, respectively. In addition, 27 SNPs led to non-synonymous mutations, and 1 SNP led to premature termination of transcription due to the presence of a stop codon (stop gain) (Figure 6B and Data Set S2). Within the candidate region, 16 genes were predicted based on the B73 V4 version reference genome of the MaizeGDB website (https://www.maizegdb.org/, accessed on 29 August 2024), including 9 genes with exons of variable sequence caused by SNPs or InDel (Figure 6D and Data Set S2).

To further identify the candidate genes of *qLA2-3*, transcriptome sequencing was performed to compare gene expression changes in the leaf auricle region of *qLA2-3*-NIL^{YS501} and *qLA2-3*-NIL^{LDC-1}. The thresholds of fold change >1.5 and $p < 0.05$ were used to identify significant differentially expressed genes. The results demonstrated that the expression of seven genes was not detected, the expression levels of five genes were not significantly changed, and only four genes (*Zm00001d006834*, *Zm00001d006835*, *Zm00001d006844*, and *Zm00001d006845*) had significant differences in expression levels between the two near-isogenic lines (Figures 6C and S2 and Table S2). The function of *Zm00001d006834* is unknown, but there is a significant difference in its expression level between the two near-isogenic lines, and it may play a role in the regulation of maize leaf angle. *Zm00001d006835* encodes a NUCLEAR FACTOR Y (NF-Y) A-type nuclear transcription factor, which is involved in numerous biological processes, including plant development and photoperiodic regulation [26–28]. *Zm00001d006844* and *Zm00001d006845* encode a serine/threonine-protein kinase and a nuclear export receptor protein (Exportin-t), respectively. The homologous genes in other species play a role in regulating plant development, including leaf development [29–31].

In addition, an SNP emerged in the exon region of *Zm00001d006848* in the LDC-1 inbred line, causing the premature occurrence of a stop codon (Data Set S2). Although it was not detected due to its low expression level (Table S2), it encoded an MYB

In addition, an SNP emerged in the exon region of *Zm00001d006848* in the LDC-1 inbred line, causing the premature occurrence of a stop codon (Data Set S2). Although it was not detected due to its low expression level (Table S2), it encoded an MYB transcription factor and was listed as a candidate gene because it may regulate the expression of other genes. Considering DNA sequence variation and gene expression differences, *Zm00001d006848*, *Zm00001d006834*, *Zm00001d006835*, *Zm00001d006844* and *Zm00001d006845* were considered as possible candidate genes (Figure 6D).

4. Discussion

The effect of LA on upright plant architecture is closely related to maize planting density [2,3]. To determine the main effect of QTLs controlling LA, RIL populations constructed by maize-inbred lines YS501 and LDC-1, which have a large LA variation, were used to identify QTLs controlling LA. The difference in LA between the two inbred lines was similar (Figure 1A,B), and the correlation of LA between different leaves was high (Figure 2), so the average LA was used for QTL mapping. The genetic architecture of average LA showed that the heritability of LA (89.15%) was high across three environments (Table 1), suggesting that LA was not susceptible to environmental influences. A total of 13 QTLs controlling the size of LA were detected, among which *qLA2-3* was stably expressed in three environments, and the remaining 12 QTLs were only detected in a single environment (Table 2).

Compared to QTL mapping results from other populations, *qLA1-1*, *qLA1-2*, *qLA1-3*, *qLA2-1*, *qLA2-2*, *qLA3-1*, *qLA3-2* and *qLA6-1* identified in this study overlapped with previously reported QTL loci [16,32–34]. *qLA1-1* overlapped with the *qLA-E1-1* interval situated between the markers bnlg439 and bnlg1803 [32]. *qLA1-2* coincided with the *qLA1-2* interval located between the markers umc2112 and umc1703 [16]. *qLA1-3* overlapped with *LA1b* located between the markers bnlg1331 and phi308707 [33]. *qLA2-1* was consistent with the positioning outcomes of B73 × Mo17 population [14]. *qLA2-2* overlapped with the *qFirLA2-1* interval located between the markers umc1065 and umc1637 [34]. *qLA3-1* overlapped with the *qLA-E3-1* interval positioned between the markers umc1394 and umc2257 [32]. *qLA3-2* was in line with the results of *LA3b* [33] and *qFirLA3-2* [34]. *qLA6-1* overlapped with the *qFirLA6-2* interval located between the markers bnlg1732 and umc2162 [34]. These QTLs detected in only one environment in this study were also located in the same location in different populations, suggesting that the QTL between these physical locations is relatively stable. *qLA2-3*, *qLA4-1*, *qLA5-1*, *qLA7-1* and *qLA10-1* were not reported in previous studies, which was due to differences in population genetic background or environment. The contribution rate of *qLA2-3* phenotypic variation reached 12.31%, and it was detected in all three environments, suggesting that this QTL is a stable and major QTL controlling maize LA.

Although many genes regulating maize LA have been cloned by using mutants, these mutants have extremely severe phenotypic variation and are difficult to use for maize genetic improvement [4,5,7–12]. Only a few genes have been cloned through fine cloning strategies, and these alleles have mild LA changes and can be applied to maize production [2,18–21]. The superior allele of the *UPA2* gene has been used to improve maize varieties used in production to achieve higher yields at higher planting densities [2]. However, the genes available for maize LA improvement are still limited, and it is still necessary to explore new gene alleles.

To narrow the interval of *qLA2-3*, InDel markers were developed based on the results of parental whole genome re-sequencing, and the genetic effects of *qLA2-3* were confirmed by genotype and phenotype analysis, which verified the authenticity and reliability of the QTL (Figure 3B). Molecular markers were continuously designed, and new recombinants were screened in the candidate interval. Finally, the target interval was narrowed to between the markers YS4 and YS5 with an interval size of 338.46 kb (B73 RefGen_v4 version). Between the two NILs of *qLA2-3*, the YS501 alleles reduced average LA by 2.51° (Figure 5), suggesting that this QTL may serve as a potential site for improving maize architecture.

Considering that maize is grown as a hybrid, this QTL effect needs to be further verified at the hybridisation stage.

The fine mapping interval contains a total of 16 genes based on the B73 reference genome (Table S2). Four differentially expressed genes were detected in the transcriptomic analysis of the near-isogenic lines *qLA2-3*-NIL^{YS501} and *qLA2-3*-NIL^{LDC-1} (Figure 6 and Table S2). *Zm00001d006835* encodes NF-Y A-type nuclear transcription factors and can co-form heterotrimeric complexes with NF-YB- and NF-YC-type transcription factors [26]. NF-Y transcription factors are involved in a variety of biological processes, such as abiotic stress response, seed germination, root development and photoperiodic regulation [27,28,35,36]. The NF-YC transcription factor ZmNF-YC13 is highly expressed at the base of maize leaves and is involved in the regulation of LA [37]. In addition, overexpression of certain NF-Y (OsNF-YB7, OsHAP3E and ZmNF-YC13) genes will affect the establishment of plant types, resulting in plant dwarf and leaf upright phenotypes [37–39]. In the present study, the expression of *Zm00001d006835* in *qLA2-3*-NIL^{YS501} with small LA was also significantly higher than that of *qLA2-3*-NIL^{LDC-1} with large LA. *Zm00001d006844* encodes a serine/threonine–protein kinase whose homolog in Arabidopsis is involved in chloroplast differentiation of leaves [29]. *Zm00001d006845* encodes a nuclear export receptor protein (Exportin-t), a homologous protein that primarily mediates the tRNA export pathway from the nucleus to the cytoplasm and regulates the development of leaf and inflorescence [30,31]. In addition, the function of *Zm00001d006834* is unknown and cannot be excluded, which may be involved in the regulation of plant LA. Although *Zm00001d006848* is not detected due to low expression (Table S2), the re-sequencing results show that the variation in the exon of *Zm00001d006848* in the LDC-1 inbred line leads to premature termination (Figure 6D and Data Set S2), and it encodes a MYB transcription factor that may affect other genes expression and regulate the angle size of maize leaves. These candidate genes need to be further confirmed through fine mapping and transgenic verification.

5. Conclusions

In the present study, 13 QTLs controlling maize LA were identified using a RIL population, in which *qLA2-3* was a stable and major QTL, explaining up to 12.31% phenotypic variation. InDel markers were developed based on parental re-sequencing data and were used to screen recombinants for fine mapping. The candidate region was finely mapped to the range of 338.46 kb (B73 RefGen_v4 version), which contains 16 predicted genes. The re-sequencing data and transcriptomics suggested that five candidate genes may be involved in the regulation of LA. To further analyse the role of the *qLA2-3* locus in maize genetic improvement, it is necessary to clone the gene through map-based cloning, study its biological functions, and undertake the evaluation of breeding utilisation in future research.

Supplementary Materials: The following supporting information can be downloaded at: https://www.mdpi.com/article/10.3390/agronomy14091978/s1, Figure S1: Frequency distributions of mean leaf angle above ear in the RIL population in E2 and E3 environment. The X-axis represents the range of leaf angle distribution on the ear within the RIL population, the Y-axis represents the frequency and the black line represents the normal distribution fitting curve; Figure S2: The verified results of qRT-PCR in *qLA2-3*-NIL^{YS501} and *qLA2-3*-NIL^{LDC-1}. Values are means ± SE; n = 3 (*, $p < 0.05$; **, $p < 0.01$, Student's *t* test); Table S1: List of primers; Table S2: Gene expression levels in *qLA2-3* interval in *qLA2-3*-NIL^{YS501} and *qLA2-3*-NIL^{LDC-1}; Data Set S1: All SNPs and InDel between the LDC-1 and YS501 in *qLA2-3* candidate region; Data Set S2: SNPs and InDel in the coding region between the LDC-1 and YS501 in *qLA2-3* candidate region.

Author Contributions: Formal analysis, H.L.; Investigation, Y.H. (Yonghui He), C.W., X.H., Y.H. (Youle Han) and F.L.; Resources, X.Z.; Supervision, Z.Y.; Validation, H.L.; Visualisation, F.L. and X.Z.; Writing—original draft, Y.H. (Yonghui He); Writing—review and editing, Z.Y. All authors have read and agreed to the published version of the manuscript.

Funding: This work was supported by the National Key Research and Development Program (2022YFD1201801-4), the National Natural Science Foundation of China (NSFC; 32101727, 32172054),

the JBGS [2021]002 project from the Jiangsu Government, the Natural Science Foundation of Jiangsu Province (Grants No BK20210794), the China Postdoctoral Science Foundation (2022M722701), and A Project Funded by the Priority Academic Program Development of Jiangsu Higher Education Institutions (PAPD).

Data Availability Statement: The National Center for Biotechnology Information Sequence Read Archive (https://www.ncbi.nlm.nih.gov/sra, accessed on 29 August 2024) provides RNA-Seq data and re-sequencing data under accession PRJNA1137054 and PRJNA1137052.

Conflicts of Interest: The authors declare no conflicts of interest.

References

1. Duvick, D.N. The contribution of breeding to yield advances in maize (*Zea mays* L.). In *Advances in Agronomy*; Sparks, D.L., Ed.; Elsevier Academic Press Inc.: San Diego, CA, USA, 2005; Volume 86, pp. 83–145.
2. Tian, J.; Wang, C.; Xia, J.; Wu, L.; Xu, G.; Wu, W.; Li, D.; Qin, W.; Han, X.; Chen, Q.; et al. Teosinte ligule allele narrows plant architecture and enhances high-density maize yields. *Science* **2019**, *365*, 658–664. [CrossRef]
3. Cao, Y.; Zhong, Z.; Wang, H.; Shen, R. Leaf angle: A target of genetic improvement in cereal crops tailored for high-density planting. *Plant Biotechnol. J.* **2022**, *20*, 426–436. [CrossRef] [PubMed]
4. Mantilla-Perez, M.B.; Salas Fernandez, M.G. Differential manipulation of leaf angle throughout the canopy: Current status and prospects. *J. Exp. Bot.* **2017**, *68*, 5699–5717. [CrossRef] [PubMed]
5. Wang, B.; Smith, S.M.; Li, J. Genetic Regulation of Shoot Architecture. *Annu. Rev. Plant Biol.* **2018**, *69*, 437–468. [CrossRef] [PubMed]
6. Tian, J.; Wang, C.; Chen, F.; Qin, W.; Yang, H.; Zhao, S.; Xia, J.; Du, X.; Zhu, Y.; Wu, L.; et al. Maize smart-canopy architecture enhances yield at high densities. *Nature* **2024**, *632*, 576–584. [CrossRef] [PubMed]
7. Bauer, P.; Lubkowitz, M.; Tyers, R.; Nemoto, K.; Meeley, R.B.; Goff, S.A.; Freeling, M. Regulation and a conserved intron sequence of liguleless3/4 knox class-I homeobox genes in grasses. *Planta* **2004**, *219*, 359–368. [CrossRef]
8. Walsh, J.; Waters, C.A.; Freeling, M. The maize geneliguleless2 encodes a basic leucine zipper protein involved in the establishment of the leaf blade–sheath boundary. *Genes Dev.* **1998**, *12*, 208–218. [CrossRef]
9. Moreno, M.A.; Harper, L.C.; Krueger, R.W.; Dellaporta, S.L.; Freeling, M. liguleless1 encodes a nuclear-localized protein required for induction of ligules and auricles during maize leaf organogenesis. *Genes Dev.* **1997**, *11*, 616–628. [CrossRef]
10. Strable, J.; Wallace, J.G.; Unger-Wallace, E.; Briggs, S.; Bradbury, P.J.; Buckler, E.S.; Vollbrecht, E. Maize *YABBY* Genes drooping leaf1 and drooping leaf2 Regulate Plant Architecture. *Plant Cell* **2017**, *29*, 1622–1641. [CrossRef]
11. Lewis, M.W.; Bolduc, N.; Hake, K.; Htike, Y.; Hay, A.; Candela, H.; Hake, S. Gene regulatory interactions at lateral organ boundaries in maize. *Development* **2014**, *141*, 4590–4597. [CrossRef]
12. Makarevitch, I.; Thompson, A.; Muehlbauer, G.J.; Springer, N.M. *Brd1* gene in maize encodes a brassinosteroid C-6 oxidase. *PLoS ONE* **2012**, *7*, e30798. [CrossRef] [PubMed]
13. Best, N.B.; Hartwig, T.; Budka, J.; Fujioka, S.; Johal, G.; Schulz, B.; Dilkes, B.P. *nana plant2* Encodes a Maize Ortholog of the Arabidopsis Brassinosteroid Biosynthesis Gene DWARF1, Identifying Developmental Interactions between Brassinosteroids and Gibberellins. *Plant Physiol.* **2016**, *171*, 2633–2647. [CrossRef] [PubMed]
14. Mickelson, S.M.; Stuber, C.S.; Senior, L.; Kaeppler, S.M. Quantitative Trait Loci Controlling Leaf and Tassel Traits in a B73 × Mo17 Population of Maize. *Crop Sci.* **2002**, *42*, 1902–1909. [CrossRef]
15. Li, C.; Li, Y.; Shi, Y.; Song, Y.; Zhang, D.; Buckler, E.S.; Zhang, Z.; Wang, T.; Li, Y. Genetic control of the leaf angle and leaf orientation value as revealed by ultra-high density maps in three connected maize populations. *PLoS ONE* **2015**, *10*, e0121624. [CrossRef]
16. Ding, J.; Zhang, L.; Chen, J.; Li, X.; Li, Y.; Cheng, H.; Huang, R.; Zhou, B.; Li, Z.; Wang, J.; et al. Genomic Dissection of Leaf Angle in Maize (*Zea mays* L.) Using a Four-Way Cross Mapping Population. *PLoS ONE* **2015**, *10*, e0141619. [CrossRef]
17. Tian, F.; Bradbury, P.J.; Brown, P.J.; Hung, H.; Sun, Q.; Flint-Garcia, S.; Rocheford, T.R.; McMullen, M.D.; Holland, J.B.; Buckler, E.S. Genome-wide association study of leaf architecture in the maize nested association mapping population. *Nat. Genet.* **2011**, *43*, 159–162. [CrossRef]
18. Ren, Z.; Wu, L.; Ku, L.; Wang, H.; Zeng, H.; Su, H.; Wei, L.; Dou, D.; Liu, H.; Cao, Y.; et al. ZmILI1 regulates leaf angle by directly affecting liguleless1 expression in maize. *Plant Biotechnol. J.* **2020**, *18*, 881–883. [CrossRef]
19. Cao, Y.; Zeng, H.; Ku, L.; Ren, Z.; Han, Y.; Su, H.; Dou, D.; Liu, H.; Dong, Y.; Zhu, F.; et al. ZmIBH1-1 regulates plant architecture in maize. *J. Exp. Bot.* **2020**, *71*, 2943–2955. [CrossRef]
20. Zhang, J.; Ku, L.X.; Han, Z.P.; Guo, S.L.; Liu, H.J.; Zhang, Z.Z.; Cao, L.R.; Cui, X.J.; Chen, Y.H. The *ZmCLA4* gene in the qLA4-1 QTL controls leaf angle in maize (*Zea mays* L.). *J. Exp. Bot.* **2014**, *65*, 5063–5076. [CrossRef]
21. Ku, L.X.; Zhang, J.; Guo, S.L.; Liu, H.Y.; Zhao, R.F.; Chen, Y.H. Integrated multiple population analysis of leaf architecture traits in maize (*Zea mays* L.). *J. Exp. Bot.* **2012**, *63*, 261–274. [CrossRef]
22. Ku, L.; Wei, X.; Zhang, S.; Zhang, J.; Guo, S.; Chen, Y. Cloning and characterization of a putative TAC1 ortholog associated with leaf angle in maize (*Zea mays* L.). *PLoS ONE* **2011**, *6*, e20621. [CrossRef] [PubMed]

23. Chen, J.Y.; Lu, F.; Chen, W.Y.; He, Y.H.; Liu, H.H.; Yin, Z.T. Mapping of growth period-related traits in maize. *Jiangsu Agric. Sci* **2022**, *50*, 63–68. (In Chinese) [CrossRef]
24. Liu, H.; Wang, H.; Shao, C.; Han, Y.; He, Y.; Yin, Z. Genetic Architecture of Maize Stalk Diameter and Rind Penetrometer Resistance in a Recombinant Inbred Line Population. *Genes* **2022**, *13*, 579. [CrossRef]
25. Li, H.; Handsaker, B.; Wysoker, A.; Fennell, T.; Ruan, J.; Homer, N.; Marth, G.; Abecasis, G.; Durbin, R.; 1000 Genome Project Data Processing Subgroup. The Sequence Alignment/Map format and SAMtools. *Bioinformatics* **2009**, *25*, 2078–2079. [CrossRef] [PubMed]
26. Petroni, K.; Kumimoto, R.W.; Gnesutta, N.; Calvenzani, V.; Fornari, M.; Tonelli, C.; Holt, B.F.; Mantovani, R. The Promiscuous Life of Plant NUCLEAR FACTOR Y Transcription Factors. *Plant Cell* **2012**, *24*, 4777–4792. [CrossRef]
27. Yang, Y.; Wang, B.; Wang, J.; He, C.; Zhang, D.; Li, P.; Zhang, J.; Li, Z. Transcription factors ZmNF-YA1 and ZmNF-YB16 regulate plant growth and drought tolerance in maize. *Plant Physiol.* **2022**, *190*, 1506–1525. [CrossRef]
28. Su, H.; Chen, Z.; Dong, Y.; Ku, L.; Abou-Elwafa, S.F.; Ren, Z.; Cao, Y.; Dou, D.; Liu, Z.; Liu, H.; et al. Identification of *ZmNF-YC2* and its regulatory network for maize flowering time. *J. Exp. Bot.* **2021**, *72*, 7792–7807. [CrossRef]
29. Lamberti, G.; Gügel, I.L.; Meurer, J.; Soll, J.; Schwenkert, S. The Cytosolic Kinases STY8, STY17, and STY46 Are Involved in Chloroplast Differentiation in Arabidopsis. *Plant Physiol.* **2011**, *157*, 70–85. [CrossRef]
30. Park, M.Y.; Wu, G.; Gonzalez-Sulser, A.; Vaucheret, H.; Poethig, R.S. Nuclear processing and export of microRNAs in *Arabidopsis*. *Proc. Natl. Acad. Sci. USA* **2005**, *102*, 3691–3696. [CrossRef]
31. Hunter, C.A.; Aukerman, M.J.; Sun, H.; Fokina, M.; Poethig, R.S. *PAUSED* Encodes the Arabidopsis Exportin-t Ortholog. *Plant Physiol.* **2003**, *132*, 2135–2143. [CrossRef]
32. Zhang, Z.; Liu, P.; Jiang, F.; Chen, Q.; Zhang, Y.; Wang, X.; Wang, H. QTL mapping for leaf angle and leaf orientation in maize using a four-way cross population. *J. China Agric. Univ.* **2014**, *19*, 7–16. (In Chinese)
33. Lu, M.; Zhou, F.; Xie, C.; Li, M.; Xu, Y.; Warburton, M.; Zhang, S. Construction of a SSR linkage map and mapping of quantitative trait loci (QTL) for leaf angle and leaf orientation with an elite maize hybrid. *Hereditas* **2007**, *29*, 1131–1138. (In Chinese) [CrossRef]
34. Chang, L.; He, K.; Liu, J.; Xue, J. Mapping of QTLs for leaf angle in maize under different environments. *J. Maize Sci.* **2016**, *24*, 49–55. (In Chinese) [CrossRef]
35. Zhang, M.; Zheng, H.; Jin, L.; Xing, L.; Zou, J.; Zhang, L.; Liu, C.; Chu, J.; Xu, M.; Wang, L. miR169o and ZmNF-YA13 act in concert to coordinate the expression of ZmYUC1 that determines seed size and weight in maize kernels. *New Phytologist* **2022**, *235*, 2270–2284. [CrossRef] [PubMed]
36. Su, H.; Cao, Y.; Ku, L.; Yao, W.; Cao, Y.; Ren, Z.; Dou, D.; Wang, H.; Ren, Z.; Liu, H.; et al. Dual functions of ZmNF-YA3 in photoperiod-dependent flowering and abiotic stress responses in maize. *J. Exp. Bot.* **2018**, *69*, 5177–5189. [CrossRef]
37. Mei, X.; Nan, J.; Zhao, Z.; Yao, S.; Wang, W.; Yang, Y.; Bai, Y.; Dong, E.; Liu, C.; Cai, Y. Maize transcription factor ZmNF-YC13 regulates plant architecture. *J. Exp. Bot.* **2021**, *72*, 4757–4772. [CrossRef] [PubMed]
38. Das, S.; Parida, S.K.; Agarwal, P.; Tyagi, A.K. Transcription factor OsNF-YB9 regulates reproductive growth and development in rice. *Planta* **2019**, *250*, 1849–1865. [CrossRef]
39. Ito, Y.; Thirumurugan, T.; Serizawa, A.; Hiratsu, K.; Ohme-Takagi, M.; Kurata, N. Aberrant vegetative and reproductive development by overexpression and lethality by silencing of OsHAP3E in rice. *Plant Sci.* **2011**, *181*, 105–110. [CrossRef]